

Xenopus TRPN1 (NOMPC) localizes to microtubule-based cilia in epithelial cells, including inner-ear hair cells

Jung-Bum Shin^{*†}, Dany Adams^{†‡}, Martin Paukert^{†§¶||}, Maria Siba^{§¶**}, Samuel Sidi^{††‡‡}, Michael Levin[‡], Peter G. Gillespie^{*§§}, and Stefan Gründer^{§¶††**§§}

^{*}Oregon Hearing Research Center and Vollum Institute, Portland, OR 97239; [‡]Department of Cytokine Biology, The Forsyth Institute, and Department of Developmental and Craniofacial Biology, Harvard Medical School, Boston, MA 02115; [§]Department of Otolaryngology, University of Tübingen, Elfriede-Aulhorn-Strasse 5, 72076 Tübingen, Germany; [¶]Department of Physiology II, University of Tübingen, Gmelinstrasse 5, 72076 Tübingen, Germany; ^{††}Max-Planck Institut für Entwicklungsbiologie, Spemannstrasse 35, 72076 Tübingen, Germany; and ^{**}Department of Physiology II, University of Würzburg, Röntgenring 9, 97070 Würzburg, Germany

Edited by Jeremy Nathans, The Johns Hopkins University School of Medicine, Baltimore, MD, and approved July 19, 2005 (received for review March 23, 2005)

In vertebrates, the senses of hearing and balance depend on hair cells, which transduce sounds with their hair bundles, containing actin-based stereocilia and microtubule-based kinocilia. A long-standing question in auditory science is the identity of the mechanically sensitive transduction channel of hair cells, thought to be localized at the tips of their stereocilia. Experiments in zebrafish implicated the transient receptor potential (TRP) channel NOMPC (drTRPN1) in this role; TRPN1 is absent from the genomes of higher vertebrates, however, and has not been localized in hair cells. Another candidate for the transduction channel, TRPA1, apparently is required for transduction in mammalian and nonmammalian vertebrates. This discrepancy raises the question of the relative contribution of TRPN1 and TRPA1 to transduction in nonmammalian vertebrates. To address this question, we cloned the TRPN1 ortholog from the amphibian *Xenopus laevis*, generated an antibody against the protein, and determined the protein's cellular and subcellular localization. We found that TRPN1 is prominently located in lateral-line hair cells, auditory hair cells, and ciliated epidermal cells of developing *Xenopus* embryos. In ciliated epidermal cells TRPN1 staining was enriched at the tips and bases of the cilia. In saccular hair cells, TRPN1 was located prominently in the kinociliary bulb, a component of the mechanosensory hair bundles. Moreover, we observed redistribution of TRPN1 upon treatment of hair cells with calcium chelators, which disrupts the transduction apparatus. This result suggests that although TRPN1 is unlikely to be the transduction channel of stereocilia, it plays an essential role, functionally related to transduction, in the kinocilium.

ciliary | mechanosensory | transduction | transient receptor potential channel

The senses of hearing and balance depend on the operation of hair cells in the inner ear and, in aquatic vertebrates, the lateral line (for review see ref. 1). Hair cells bear microscopically fine projections, the stereocilia, on their apical surfaces; these stereocilia contain actin filaments and are grouped in hair bundles. Individual stereocilia within a bundle are connected by different types of links, most notably the tip links, which interconnect the tips of the stereocilia. Most hair cells, with the exception of those from the hearing organs of mammals and birds, contain on their apical surface in addition to the stereocilia one kinocilium, which is coupled to the hair bundle by kinociliary links. The kinocilium is a true cilium containing a (9 + 2) arrangement of microtubules, similar to motile cilia. The displacement of the hair bundle by mechanical forces increases tension in the tip links, opening the mechanotransduction channels and depolarizing the hair cell. In frog hair cells, the mechanical forces are delivered through the kinocilium to the stereocilia (2).

The transduction channels of vertebrate hair cells are nonselective cation channels with a high permeability to Ca²⁺ (3–5). They are blocked by micromolar concentrations of ruthenium red (6) and allow the passage of the small fluorescent dye FM 1-43 (7, 8). These characteristics make ion channels of the transient receptor potential (TRP) family good candidates for the transduction channel (9, 10). Recently, functional evidence has accumulated that implicates TRP channels in transduction. Analysis of mutant flies in which the sensory bristles had mechanoreceptor potentials of diminished amplitude revealed that some of these flies had a defect in a gene called *nompC* (11). The protein encoded by *nompC* is a TRP channel, now called TRPN1, characterized by 29 ankyrin repeats at its intracellular N terminus (11). A TRPN1 ortholog is present in zebrafish; morpholino-mediated removal of TRPN1 function eliminated electrical responses in zebrafish hair cells, resulting in larval deafness and imbalance (12). Although the analysis of TRPN1-deficient flies and zebrafish indicated that TRPN1 is essential for mechanotransduction in these organisms, evidence for its cellular and subcellular location in mechanosensitive organs was lacking.

One puzzle with TRPN1 is that it is apparently absent from the completely sequenced genomes of higher vertebrates such as humans and mice (12). Very recently, another TRP channel, TRPA1 (formerly known as ANKTM1), was proposed as a transduction channel of both lower and higher vertebrates (13). This finding questioned the relative importance of TRPA1 and TRPN1 for transduction in lower vertebrates. To address this question, we cloned the TRPN1 ortholog from the amphibian *Xenopus laevis* and investigated its cellular and subcellular location. Our results show that TRPN1 is prominently expressed at the tip of the kinocilium, consistent with an essential role in hair-cell function (12), but in kinocilia instead of stereocilia.

Materials and Methods

Cloning of xTRPN1. We compared the coding sequences of *Danio*, *Drosophila*, and *Caenorhabditis* TRPN1 and used conserved

This paper was submitted directly (Track II) to the PNAS office.

Abbreviations: TRP, transient receptor potential; Cdh23, cadherin 23; IFT, intraflagellar transport.

Data deposition: The sequence reported in this paper has been deposited in the GenBank database (accession no. AJ576027).

[†]J.-B.S., D.A., and M.P. contributed equally to this work.

[¶]Present address: Department of Neuroscience, The Johns Hopkins University School of Medicine, Baltimore, MD 21205.

^{**}Present address: Department of Pediatric Oncology, Dana-Farber Cancer Institute, Harvard Medical School, Boston, MA 02115.

^{§§}To whom correspondence may be addressed. E-mail: gillespp@ohsu.edu or stefan.gruender@mail.uni-wuerzburg.de.

© 2005 by The National Academy of Sciences of the USA

regions to design PCR primers nompC-H1644-u (5'-CAY-CAYYTRTTTCGGVCCITGGGC-3') and nompC-R1785-l (5'-CGCTGRTAKGTRTCRCTCATCAT-3'). Poly(A)⁺ RNA was isolated from stage V–VI oocytes of *X. laevis* and reverse-transcribed (SuperScript reverse transcriptase; Invitrogen). Using this cDNA as a template, a 390-bp PCR product showing homology with other TRPN1 genes was obtained. This PCR product was extended in four consecutive rounds of 5'-RACE and one round of 3'-RACE. RACE was performed by using the Smart RACE cDNA amplification kit (Clontech) with RNA from oocytes or spleen of an adult *Xenopus* female. PCR products were subcloned with the TOPO-TA cloning kit (Invitrogen) and sequenced. Full-length xlTRPN1 (GenBank accession no. AJ576027) was assembled from the different RACE products. The presence of a stop codon upstream of the methionine was confirmed in independent RACE reactions with different sets of primers.

Generation of xlTRPN1 Antiserum. A synthetic peptide (CIPVN-VKGKFSST) corresponding to the C terminus of xlTRPN1 was coupled by its cysteine to keyhole limpet hemocyanin and used to raise a polyclonal antiserum in rabbits (Charles River Laboratories). Interestingly, the C-terminal sequence was not present in bullfrog TRPN1 (J.-B.S. and P.G.G., unpublished data). The antiserum was purified by affinity chromatography with the synthetic peptide.

Immunostaining of *Xenopus* Embryos. Embryos were raised in 0.1× Marc's modified Ringer's (MMR) solution (10 mM NaCl/0.2 mM KCl/0.2 mM CaCl₂/0.5 mM Hepes/0.1 mM MgCl₂/0.01 mM EDTA, pH 7.8) without the standard gentamicin supplementation. Embryo batches, in which the lateral-line cells were to be selectively killed, were exposed to 1 mM neomycin in 0.1× MMR from stage 31 to stage 48. For immunohistochemistry, embryos were fixed with MEMFA (3.7% formaldehyde in 1× MEM salts) at stage 48 and stored in 1× PBS with 0.1% sodium azide. Before immunohistochemistry, embryos were incubated in PBS plus 1% Triton X-100 for 20 min. Embryos were then blocked with PBT-BSA (PBS containing 0.1% Tween 20 and 1% BSA) plus 10% goat serum. The TRPN1 primary antibody was used at 4 μg/ml, followed by PBS-BSA washes (six times, 1 h each). An alkaline phosphatase-conjugated anti-rabbit secondary antibody was applied at a dilution of 7.5 μg/ml, followed by washes (six times, 1 h each), and detected by using the standard 5-bromo-4-chloro-3-indolyl phosphate/nitroblue tetrazolium substrate. The negative controls were performed in exactly the same protocol, except that the primary antibody was preadsorbed with excess (1 mg/ml) TRPN1 peptide, rocking at 4°C overnight before addition to the embryos.

Immunostaining of *Xenopus* Sacculi. *Xenopus* sacculi were dissected in a saline solution (containing 110 mM NaCl, 2 mM KCl, 2 mM MgCl₂, 3 mM D-glucose, and 10 mM Hepes, pH 7.25) with 4 mM CaCl₂. Sacculi were incubated in 75 μg/ml protease XXIV (Sigma) for 10 min to allow removal of the otolithic membrane with fine forceps. For EGTA treatment, tissues were incubated for 30 min in 5 mM EGTA in saline. All samples were washed three times in PBS and fixed for 25 min with 3% formaldehyde in PBS. After blocking for 1 h with 1% BSA, 3% normal donkey serum, and 0.2% saponin in PBS, samples were incubated with primary antibodies overnight at room temperature in blocking buffer. Rabbit anti-xlTRPN1 was used at 2 μg/ml, and monoclonal anti-α-tubulin (Sigma) was used at 1:500. The blocking peptide was used in a concentration of 1 μM. After washing 3 × 5 min with PBS, samples were incubated with secondary antibodies (7.5 μg/ml Cy3-conjugated donkey anti-rabbit IgG and Cy5-conjugated donkey anti-mouse IgG; Jackson ImmunoResearch Laboratories) and 0.25 μM FITC-phalloidin (Sigma) in

the blocking solution for 1–3 h. Finally, organs were washed five times in PBS and mounted in Vectashield (Vector Laboratories). To obtain profile views from hair bundles, sacculi were mechanically disrupted by using a fine forceps while tissues were in Vectashield. Samples were viewed with Plan Apochromat ×60 (numerical aperture, 1.40) oil lenses on a Nikon TE 300 inverted microscope with a Bio-Rad MRC 1024 confocal imaging system.

Amplification Protocol. A modified version of the Vectastain ABC kit protocol for rabbit IgG was used (Vector Laboratories). Primary steps of the protocol were identical to the staining protocol described above. After overnight incubation with the primary antibody (antibody concentration 0.67 μg/ml) at room temperature, sacculi were washed three times in PBS and incubated in a solution containing biotinylated anti-rabbit IgG (prepared according to the ABC kit) for 1 h. Then the tissue was washed three times in PBS, incubated for 30 min in the ABC reagent made up according to the ABC kit, washed again, and incubated again in diluted biotinylated tyramine for 10 min. After three more PBS washes, the samples were incubated in PBS containing streptavidin-Cy5 (7.5 μg/ml) and 0.25 μM FITC-Phalloidin for 1 h. Finally, samples were washed five times in PBS and mounted in Vectashield (Vector Laboratories).

Results

Cloning of TRPN1 from *X. laevis*. We isolated a cDNA for the TRPN1 (or NOMPC) ortholog from *X. laevis* by homology cloning (see *Materials and Methods*). The TRPN1 cDNA clone encodes a 1,521-aa protein with a predicted molecular mass of 168 kDa. *Xenopus* and zebrafish TRPN1 are 63% identical at the amino acid level, whereas *Xenopus* and *Drosophila* TRPN1 are 43% identical (Fig. 4, which is published as supporting information on the PNAS web site). xlTRPN1 has a long N terminus with 28 ankyrin repeats. By contrast, TRPN1 from zebrafish and *Drosophila* contain 29 ankyrin repeats; the most N-terminal ankyrin repeat is missing from xlTRPN1 (Fig. 4). The ankyrin repeats of xlTRPN1 are followed by six predicted transmembrane domains (S1–S6) and a short C terminus.

Phylogenetic analysis (Fig. 5, which is published as supporting information on the PNAS web site) indicates that TRPN1 is only distantly related to other TRP channels; the closest relatives are the TRPC and TRPM channels. Moreover, there is no evidence for a second TRPN1 channel from *Xenopus* and zebrafish EST and genomic databases or from the complete *Drosophila* genome, suggesting that there is only one member of the TRPN1 family in each of these organisms. Because formation of heteromeric channels is usually confined to subunits within a subfamily (14, 15), it is likely that TRPN1 forms a homomultimeric channel.

We raised an antibody against the C terminus of xlTRPN1 and purified the antiserum against the peptide that was used for immunization. Immunoblot analysis of xlTRPN1 heterologously expressed in *Xenopus* oocytes revealed a single crossreactive protein with an apparent molecular mass of ≈170 kDa (Fig. 6, which is published as supporting information on the PNAS web site).

Localization of TRPN1 in *Xenopus* Embryos. We investigated the distribution of xlTRPN1 in different tissues by immunohistochemistry. First, we examined the lateral line, part of the sense of equilibrium of tadpoles. We used the dye FM1-43, which passes through open transduction channels (7, 8), to detect lateral-line hair cells (16) in the head of stage-45 (corresponding to ≈4.5 days postfertilization) *Xenopus* embryos (Fig. 1*A* and *C*). Staining with the anti-TRPN1 antibody revealed specific localization of TRPN1 to the arc of lateral-line stitches surrounding the eye, as well as the neurons surrounding the nostrils (Fig. 1*E* and *G*). We determined whether stained cells in the lateral line

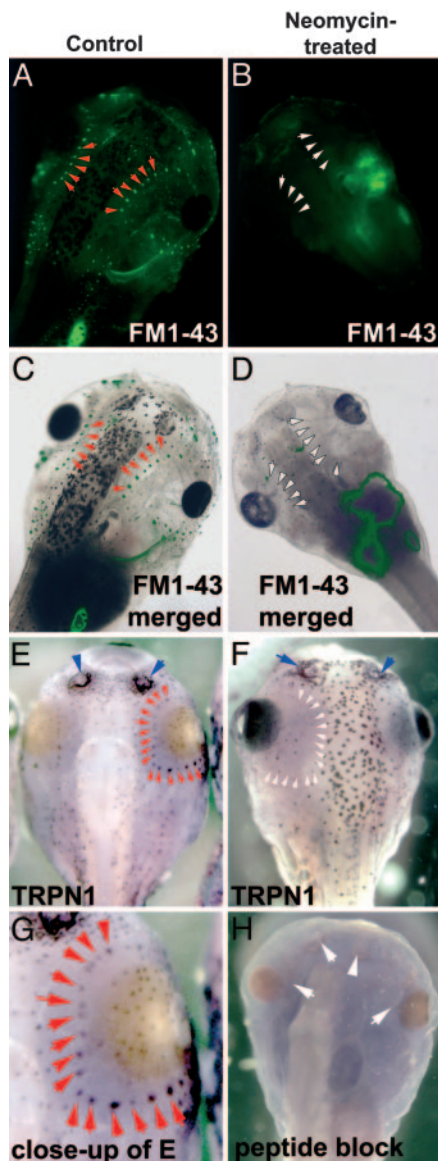


Fig. 1. Localization of TRPN1 in lateral-line hair cells of stage-45 *Xenopus* embryos. (A and B) Dissecting microscope dorsal view of embryos that had been stained with FM1-43 to label lateral-line hair cells. In A, red arrows point to lateral-line hair cells around the eye; in B, white arrows highlight the absence of FM1-43 staining around the eyes of neomycin-treated embryos. (C and D) Shown are A and B merged with their respective transmitted light images to better show the localization of FM1-43 staining. (E) Staining with the anti-TRPN1 antibody. Dorsal view of an embryo that had been bleached to distinguish alkaline phosphatase staining from pigment. Red arrows point to staining of the lateral-line stitches around the eye. Blue arrows point to staining of the nostrils. (F) Anti-TRPN1 staining of unbleached, neomycin-treated embryo. Nostrils are positive for TRPN1, but staining around the eyes is absent, showing that the neomycin effect is specific to lateral-line hair cells. (G) Close-up of the lateral-line staining surrounding the eye shown in E. Red arrows point to signal in lateral-line stitches. (H) Dorsal view of bleached embryo. Preadsorption of the TRPN1 antibody with the epitope peptide prevented TRPN1 staining of both the lateral line and the nostril (white arrows).

corresponded to sensory hair cells by treating the embryos with the aminoglycoside antibiotic neomycin, which specifically destroys hair cells (17). FM1-43 staining revealed that the lateral-line hair cells were indeed absent from neomycin-treated embryos (Fig. 1 B and D). In these embryos, the TRPN1 staining

in the arc of stitches surrounding the eye was also absent (although nostril staining remained, as an internal positive control; Fig. 1F), indicating that TRPN1 is expressed in the lateral-line hair cells. The staining was specific for TRPN1, because it could be prevented by preincubating the antibody with the epitope peptide (Fig. 1H).

In addition to lateral-line hair cells, a population of cells that are evenly distributed over the whole surface of the embryo was strongly stained by the anti-TRPN1 antibody (Fig. 2B), whereas another population of epidermal cells was more weakly stained (Fig. 2B). Sectioning confirmed the predicted cell-membrane localization of TRPN1 in these cells (Fig. 2C). Preincubating the antibody with the immunogenic peptide completely prevented this staining (Fig. 2A). The distribution of TRPN1-positive cells resembled the distribution of ciliated epidermal cells, which contain motile cilia characterized by a (9 + 2) arrangement of microtubules (18, 19). We investigated whether the stained cells in the epidermis correspond to ciliated cells by staining the embryos with an antibody against α -tubulin, a principal component of cilia. Overlaying the images obtained with the anti-TRPN1 antibody (Fig. 2D) and the anti- α -tubulin antibody (Fig. 2E) revealed that both antibodies stained the same cells in 100% of the embryos examined (Fig. 2F). We then examined each cell at high magnification. Transmitted light photography revealed the tuft of cilia on the surface of a ciliated cell (Fig. 2G). These cilia were stained by TRPN1 (Fig. 2H) and confirmed as cilia by α -tubulin staining (Fig. 2I). Merging the views revealed 100% overlap (Fig. 2J), showing that TRPN1 is present specifically on cilia. High magnification revealed that whereas TRPN1 protein was present throughout the surface of the cilia, there were specific nodes on each cilium, especially at its bottom (Fig. 2K), close to the basal body, and at its tip (Fig. 2L and M), where TRPN1 was highly enriched.

Localization of TRPN1 in *Xenopus* Sacculi. Finally, we addressed whether TRPN1 is expressed in the inner ear of *Xenopus*. The frog inner ear consists of the sacculus, the utricle, the semicircular canals, and the lagena. The most prominent of these organs is the sacculus, which detects vertical linear acceleration with its $\approx 2,500$ mechanosensitive hair cells (20). Because hair cells residing in the frog sacculus are significantly larger than those in many other organisms, they provide an excellent model to study the localization of TRPN1 protein in hair cells at high resolution. Whole mounts of *Xenopus* sacculi were labeled with the anti-TRPN1 antibody. The strongest signal was seen in the tip of the kinocilium, at the bulb that marks the end of this process (Fig. 3A). Sparse punctate staining was also observed in cell bodies of hair cells and supporting cells. The specificity of the staining was confirmed by preincubating the antibody with the epitope peptide (Fig. 3B); kinocilial bulb immunoreactivity was fully prevented, but cell body labeling was only slightly diminished. We found similar TRPN1 immunolocalization in the utricle and the lagena (data not shown). To examine low-level TRPN1 expression, we used an amplification protocol that used biotinylated tyramine, peroxidase, and fluorescent streptavidin (21). Using this method, we were unable to detect TRPN1 at stereocilia tips (data not shown). We conclude from these experiments that TRPN1 is abundant in the kinocilial bulb but is probably not present at stereocilia tips at significant levels.

If TRPN1 is essential for transduction in frog hair cells but present in kinocilia, it may couple mechanically with kinocilial links, recently identified as cadherin 23 (Cdh23) (22, 23). In frog hair cells, kinocilial links connect the kinocilium to the two to six tallest stereocilia at the kinocilial bulb (24). TRPN1 labeling was adjacent to strong labeling for Cdh23 in kinocilial links, although Cdh23 was clearly present in stereocilia and TRPN1 in kinocilia (Fig. 3 C and D). Kinocilial link cleavage

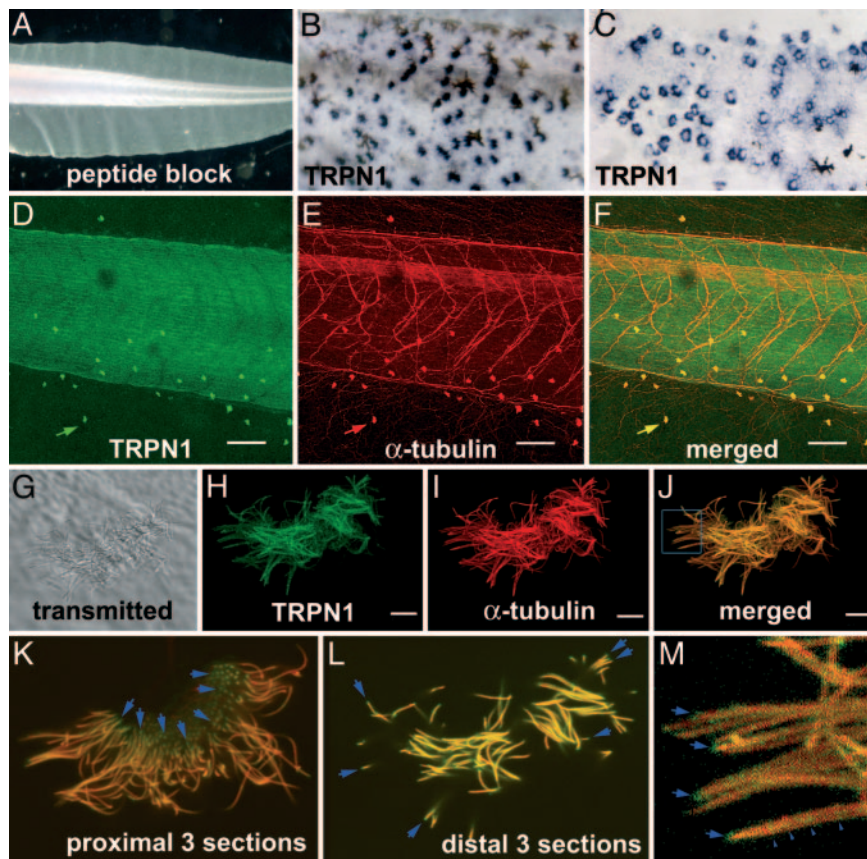


Fig. 2. Localization of TRPN1 in cilia of epidermal cells. (A) Bleached tail from a control tadpole. Preadsorption of the anti-TRPN1 antibody with the epitope peptide prevented TRPN1 staining in the epidermis of embryos. (B) Staining of epidermal cells by the anti-TRPN1 antibody (dark blue spots). Full panel width is $\approx 600 \mu\text{m}$. (C) Planar sections through epidermal tissue showing TRPN1 staining in open circles, consistent with the predicted cell-membrane localization of TRPN1. Full panel width is $\approx 600 \mu\text{m}$. (D–F) Fluorescence of doubly labeled tadpole tails. Maximal projections of z-series. (D) TRPN1 (FITC). (E) α -Tubulin (TRITC). (F) Merged images. TRPN1 stain is seen in bright spots (e.g., green arrow); green hue in muscle in D is autofluorescence. α -Tubulin is brightest in neurons and ciliated cells (e.g., red arrow). The merged image shows that the TRPN1 and α -tubulin are colocalized in the ciliated cells (yellow arrow). (G–J) Higher-magnification images of the cilia of epidermal cells. (G) Transmitted light image, single section from confocal z-series showing the cilia. (H) TRPN1. (I) α -Tubulin in the cilia shown in G, maximum projection of z-series. (J) H and I merged, showing colocalization of TRPN1 and tubulin in cilia. Blue box indicates approximate boundaries of high magnification shown in M. (K) Projection of three proximal sections from J. (L) Projection of three sections from J showing the distal ends of cilia. Blue arrows point to some of the visible cilia tips; both the proximal and the distal ends of cilia stain more heavily for TRPN1. (M) Very high magnification of some cilia distal tips, corresponding to the box in J. The z-series used to create J was restored by using Wiener deconvolution, a process that removes artifactual light from images collected at this high magnification. PHOTOSHOP (Adobe Systems, San Jose, CA) was then used to increase the resolution (bicubic) and increase contrast. Blue arrows point to the tips where TRPN1 is concentrated. Punctate TRPN1 staining is also visible along the cilia. (Scale bars: $200 \mu\text{m}$, D–F; $8 \mu\text{m}$, G–J.) (Full width: $70 \mu\text{m}$, K–L; $20 \mu\text{m}$, M.)

may release the channel from its mechanical restraints and could result in its relocation within hair cells. Calcium chelators like EGTA and 1,2-bis(2-aminophenoxy)ethane- N,N,N',N' -tetraacetate (BAPTA) cleave not only tip links, but kinocilial links as well (25). Indeed, after EGTA treatment (5 mM, 30 min), TRPN1 immunoreactivity at the kinocilial bulb was reduced in intensity; simultaneously, immunoreactivity appeared at the base of the kinocilium (Fig. 3 E–O), resembling the relocation of Cdh23 signal in the bullfrog (22). We confirmed that EGTA treatment relocates Cdh23 labeling in *Xenopus* hair cells (data not shown), comparable to the findings described for bullfrog hair cells (22).

Discussion

We demonstrate here that TRPN1 (or NOMPC) is present in the mechanoreceptive organs of *Xenopus*, the lateral-line and vestibular hair cells, further supporting the idea that it is essential for mechanotransduction in hair cells of some vertebrates. Within hair cells, TRPN1 is highly abundant in the terminal bulbs of the microtubule-based kinocilia. Moreover, the relocation of TRPN1 staining after EGTA treatment is

consistent with it sharing properties with the transduction apparatus. Our data do not support the hypothesis that TRPN1 is expressed at the tips of the actin-based stereocilia. Because another TRP channel, TRPA1, localizes to the tips of the stereocilia in the bullfrog (13), it is reasonable to conclude that TRPA1 but not TRPN1 is the main transduction channel of frog stereocilia. This conclusion contrasts with the complete deafness induced in zebrafish injected with morpholino oligonucleotides that suppress TRPN1 expression (12). Although it is possible that TRPN1 also plays a role in stereocilia in zebrafish or that transduction there occurs in kinocilia, it seems more likely that the essential role for TRPN1 is in the kinocilium. However, when microdissected from the rest of the bundle, kinocilia do not transduce; moreover, the receptor potential of hair cells lacking a kinocilium is not noticeably less than one with a kinocilium (26). Although functional data are lacking, it is nevertheless plausible that when attached to stereocilia, kinocilia carry a small TRPN1-mediated transduction current. Alternatively, a role for TRPN1 might not even require channel function; perhaps TRPN1 is the receptor in the kinocilium for the Cdh23 filaments that make up the

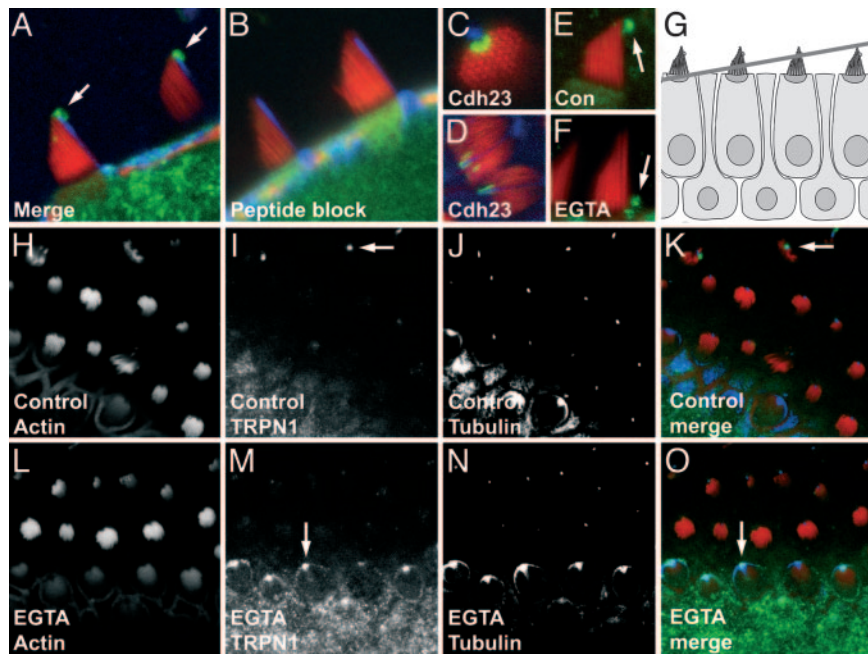


Fig. 3. Localization of TRPN1 in *Xenopus* vestibular hair cells. (A) Saccular hair cells in profile. Triple staining for TRPN1 (green), actin (red), and tubulin (blue); pseudocolor code also applies to B, E, F, K, and O. Arrows indicate TRPN1 at the kinocilia bulb. (B) Preincubation of the TRPN1 antibody with the epitope peptide prevents TRPN1 staining at the kinocilia tip. (C and D) Cdh23 (green), actin (red), and tubulin (blue) in hair cell under control conditions. Cdh23 is present in the two to six tallest stereocilia in a stripe adjacent to the kinocilia bulb. (E) TRPN1 and actin in hair cell under control conditions. Note TRPN1 in kinocilia bulb (arrow). (F) After EGTA treatment (5 mM, 30 min), the TRPN1 signal appears at the base of the kinocilium (arrow). (G) Graphic illustration of the optical section in the confocal sections of H–O. (H–O) Whole-mount view of hair bundles, in a slightly angular optical section as illustrated in G. (H–K) Control conditions. (H) Actin. (I) TRPN1. (J) Tubulin. (K) Merged signals. (L–O) After EGTA treatment. (L) Actin. (M) TRPN1. (N) Tubulin. (O) Merged signals. Full panel widths: 24 μm , A and B; 8 μm , C; 25 μm , D; 13 μm , E and F; 45 μm , H–O.

kinocilia links, which are essential for propagation of forces to the stereocilia.

Expression of TRPN1 in the beating cilia of the ciliated cells of the larval epidermis was unexpected. Ciliated cells originate from the inner sensory layer of the bilayered epidermis and become visible on the surface of the embryos early in development (≈ 18 h after fertilization), disappearing during metamorphosis (27). The function of ciliated cells is enigmatic but it has been proposed that by beating in the same direction they could generate directed fluid flow in the intravitelline medium (28). The expression of TRPN1 in these cilia is reminiscent of the expression of another TRP channel, TRPP2 (also known as polycystin-2 or PKD2), in primary cilia of kidney cells (29, 30). It has been proposed that the kidney primary cilium is a sensory organelle, monitoring the rate of fluid flow through the kidney tubules (31). TRPP2 may mediate Ca^{2+} influx into the cilium upon mechanical bending of the cilium (32). We speculate that TRPN1 serves a similar role in the cilia of epidermal ciliated cells. The presence of TRPN1 in motile cilia of the frog larval epidermis and in the kinocilium of frog hair cells, its apparent absence from stereocilia of frog hair cells, and its required role in transduction carried out by microtubule-based mechanosensory neurons of fly bristles (11) together suggest that TRPN1 is restricted to true cilia.

Interestingly, we found TRPN1 not only concentrated at the tips of the epidermal cilia, consistent with a sensory function, but also at their base. Cilia depend for their assembly and maintenance on a specialized transport system, known as intraflagellar transport (IFT) (31). In *Chlamydomonas*, IFT particles are localized primarily to the base of the cilium, whereas only a few particles, probably representing those in transit, are in the cilium (33). We speculate that the strong TRPN1 staining at the base of the cilium reflects its association with IFT particles, whereas

the punctate staining along the length of the cilium may reflect IFT particles containing TRPN1 in transit. This hypothesis would predict that there is intense transport of TRPN1 to the tip of the cilium, indicating a high turnover of this protein. Likewise, the strong immunoreactivity at the base of the kinocilium after hair cells are treated with calcium chelators may reflect IFT particles destined for the distal end of the kinocilium, bearing TRPN1 molecules for repair of the damaged linkage.

From analysis of presently available sequence databases, TRPN1 is not present in the genomes of birds and mammals. In contrast, TRPA1 is present in the genomes of birds and mammals as well as fishes and amphibians (13). Thus, TRPN1 and TRPA1 coexist in lower vertebrate species, suggesting that lower vertebrates have two channels that could mediate transduction. Higher vertebrates preserved only one of them, TRPA1, whereas TRPN1 vanished during evolution. Therefore, it seems that TRPN1 served a function in lower vertebrates that became dispensable in higher vertebrates. At present, we can only speculate about this function of TRPN1 but its strong expression in true cilia argues for a specialized function of TRPN1 there. Nevertheless, our results both support the idea that TRPN1 plays an essential role in hair-cell transduction and increase our understanding of the molecular evolution of transduction mechanisms in vertebrate hair cells.

We thank Teresa Nicolson for sharing the zebrafish TRPN1 sequence before publication, urging us to advance with this project, and participating in many helpful discussions; Ulrich Müller (The Scripps Research Institute, La Jolla, CA) for providing the Cdh23 antibody; Shing-Ming Cheng for assistance with immunohistochemistry; and Debra Sorocco, Punita Koustubhan, and Adam Crook for *Xenopus* husbandry. This work was supported by National Institutes of Health Grants R01 DC002368 (to P.G.G.), P30 DC005983 (to P.G.G.), R01 GM06227 (to M.L.), and T32-DE-07327 (to D.A.) and American Cancer Society Grant RSG-02-046-01-DDC (to M.L.).

1. Gillespie, P. G. & Walker, R. G. (2001) *Nature* **413**, 194–202.
2. Jacobs, R. A. & Hudspeth, A. J. (1990) *Cold Spring Harbor Symp. Quant. Biol.* **55**, 547–561.
3. Corey, D. P. & Hudspeth, A. J. (1979) *Nature* **281**, 675–677.
4. Ohmori, H. (1985) *J. Physiol. (London)* **359**, 189–217.
5. Lumpkin, E. A., Marquis, R. E. & Hudspeth, A. J. (1997) *Proc. Natl. Acad. Sci. USA* **94**, 10997–11002.
6. Farris, H. E., LeBlanc, C. L., Goswami, J. & Ricci, A. J. (2004) *J. Physiol. (London)* **558**, 769–792.
7. Gale, J. E., Marcotti, W., Kennedy, H. J., Kros, C. J. & Richardson, G. P. (2001) *J. Neurosci.* **21**, 7013–7025.
8. Meyers, J. R., MacDonald, R. B., Duggan, A., Lenzi, D., Standaert, D. G., Corwin, J. T. & Corey, D. P. (2003) *J. Neurosci.* **23**, 4054–4065.
9. Strassmaier, M. & Gillespie, P. G. (2002) *Curr. Opin. Neurobiol.* **12**, 380–386.
10. Corey, D. P. (2003) *Neuron* **39**, 585–588.
11. Walker, R. G., Willingham, A. T. & Zuker, C. S. (2000) *Science* **287**, 2229–2234.
12. Sidi, S., Friedrich, R. W. & Nicolson, T. (2003) *Science* **301**, 96–99.
13. Corey, D. P., Garcia-Añoveros, J., Holt, J. R., Kwan, K. Y., Lin, S. Y., Vollrath, M. A., Amalfitano, A., Cheung, E. L., Derfler, B. H., Duggan, A., *et al.* (2004) *Nature* **432**, 723–730.
14. Shen, N. V. & Pfaffinger, P. J. (1995) *Neuron* **14**, 625–633.
15. Xu, J., Yu, W., Jan, Y. N., Jan, L. Y. & Li, M. (1995) *J. Biol. Chem.* **270**, 24761–24768.
16. Winklbaauer, R. (1989) *Prog. Neurobiol.* **32**, 181–206.
17. Harris, J. A., Cheng, A. G., Cunningham, L. L., MacDonald, G., Raible, D. W. & Rubel, E. W. (2003) *J. Assoc. Res. Otolaryngol.* **4**, 219–234.
18. Chu, D. T. & Klymkowsky, M. W. (1989) *Dev. Biol.* **136**, 104–117.
19. Deblandre, G. A., Wettstein, D. A., Koyano-Nakagawa, N. & Kintner, C. (1999) *Development (Cambridge, U.K.)* **126**, 4715–4728.
20. Diaz, M. E., Varela-Ramirez, A. & Serrano, E. E. (1995) *Hear. Res.* **91**, 33–42.
21. Adams, J. C. (1992) *J. Histochem. Cytochem.* **40**, 1457–1463.
22. Siemens, J., Lillo, C., Dumont, R. A., Reynolds, A., Williams, D. S., Gillespie, P. G. & Müller, U. (2004) *Nature* **428**, 950–955.
23. Söllner, C., Rauch, G. J., Siemens, J., Geisler, R., Schuster, S. C., Müller, U. & Nicolson, T. (2004) *Nature* **428**, 955–959.
24. Eatock, R. A., Corey, D. P. & Hudspeth, A. J. (1987) *J. Neurosci.* **7**, 2821–2836.
25. Goodyear, R. J. & Richardson, G. P. (2003) *J. Neurosci.* **23**, 4878–4887.
26. Hudspeth, A. J. & Jacobs, R. (1979) *Proc. Natl. Acad. Sci. USA* **76**, 1506–1509.
27. Nishikawa, S., Hirata, J. & Sasaki, F. (1992) *Histochemistry* **98**, 355–358.
28. König, G. & Hausen, P. (1993) *Dev. Biol.* **160**, 355–368.
29. Pazour, G. J., San Agustin, J. T., Follit, J. A., Rosenbaum, J. L. & Witman, G. B. (2002) *Curr. Biol.* **12**, R378–R380.
30. Yoder, B. K., Hou, X. & Guay-Woodford, L. M. (2002) *J. Am. Soc. Nephrol.* **13**, 2508–2516.
31. Rosenbaum, J. L. & Witman, G. B. (2002) *Nat. Rev. Mol. Cell. Biol.* **3**, 813–825.
32. Nauli, S. M., Alenghat, F. J., Luo, Y., Williams, E., Vassilev, P., Li, X., Elia, A. E., Lu, W., Brown, E. M., Quinn, S. J., *et al.* (2003) *Nat. Genet.* **33**, 129–137.
33. Deane, J. A., Cole, D. G., Seeley, E. S., Diener, D. R. & Rosenbaum, J. L. (2001) *Curr. Biol.* **11**, 1586–1590.